Influence of High Pressure Hydrogen Environment on Creep Deformation of Mo-Re, Haynes 188, and NARloy-Z Alloys

NASA Grant No. NAG 2-865

Annual Technical Report

S. M. L. Sastry (Principal investigator)
Charles C. Yang
Shewang Ouyang
K. L. Jerina

Washington University, St. Louis MO.

D. S. Schwartz

McDonnell Douglas Corporation, St. Louis MO.

Submitted

to

National Aeronautical and Space Administration
Attention: Barbara Hastings
ASC: 241-1
Ames Research Center
Moffet Field, CA 94035-1000

Nov 27, 1994

CONTENTS

1. INTRODUCTION

Candidate materials for potential use in hypersonic vehicles are likely to be exposed to harsh hydrogen environments at high temperatures. Studies of environmental effects on such materials are of practical value for two reasons. First, the study of the deformation behavior influenced by environment leads to a better understanding of the fundamentals of the metal-environment reactions, and, second, this information is particularly important in the selection and successful operation of materials under severe environmental service condition.

The present study focuses on the investigation of the influence of hydrogen on the mechanical properties of three type of alloys at elevated temperatures. The reasons for the consideration of hydrogen effects are the potential use of hydrogen as a coolant in gas-cooled reactors and fuel in advanced hypersonic vehicles. The materials used in hydrogen atmosphere must not be embrittled by hydrogen at ambient temperature and should have good strength in hydrogen atmosphere at elevated temperature. The paucity of information concerning the mechanical performance in hydrogen atmosphere at elevated temperature has been a limiting factor in the selection and design of structural components for operation in hydrogen environment.

The materials chosen for the present study are based on Mo-47.5Re, Co-22Ni-22Cr-15W-3Fe-1.2Mn-0.2Si (Haynes 188) and Cu-3Ag-0.5Zr (NARloy-Z) which are attractive candidates for hypersonic vehicles because for their excellent combination of high temperature strength, creep resistance and thermal conductivity. Incremental stress creep tests and stress rupture tests in inert gas and hydrogen-containing atmospheres at elevated temperatures are used to determine the hydrogen effects on creep behavior. The test specimens are examined by optical metallography and scanning electron microscopy before and after testing. All creep-rupture data are analyzed to determine the parameters that dominate the deformation mechanisms for different alloys for various testing

conditions and for determining the hydrogen effects on material properties at elevated temperature.

2. BACKGROUND

Hydrogen is increasingly being used as a coolant and fuel in the advanced rocket propulsion engines. The materials used in such hydrogen atmosphere must not be embrittled by hydrogen in ambient temperature and must maintain good strength in hydrogen atmosphere at elevated temperature.

When hydrogen comes in contact with metals, it ionizes immediately due to the potential field of metals. The nature of the ionization varies with materials. The ionized hydrogen can be negatively charged ion (H^-) or a positively charged (proton). The negatively charged ions form chemical compounds having ionic bonds and new specific lattice. These chemical compounds lose their original metallic properties. This type of interaction is the characteristic of alkali metals, like the hydride formation of LiH and NaH, etc.

When hydrogen atom is ionized as a proton, it enters the metal lattice without changing metal's original properties. Protons are so small that they can move readily in the metal lattice. The proton gas permeates the electron shell of the metallic atoms and cause some change in the energy level of the metals. This is evidenced by the reduction of melting temperature of copper and nickel and the reduction of phase transformation temperatures of titanium (1).

The second type of reaction is our main concern. The majority of interest and study of hydrogen effects on mechanical properties of metals have been with respect to hydrogen embrittlement and many comprehensive reviews have been published on this subject. The subject of hydrogen embrittlement is briefly discussed below since it is of general applicability. The most frequently encountered hydrogen embrittlements processes are as follows:

1. The hydrides formed in Ti and Zr alloys are brittle and serve as crack initiation sites as well as barriers to movement of dislocations (2,3).
2. Low strain rate embrittlement in Fe- and Ni-based alloys caused by hydrogen enhanced localized plasticity (4,5).
3. "Hydrogen attack" in carbon steel wherein hydrogen reacts with carbon to form methane gas that expands and disrupts the materials (6).
4. "Hydrogen disease" in copper wherein hydrogen reacts with entrapped oxygen or oxide inclusions to form water vapor (7).

The main objective of the present study is a study of hydrogen degradation effects at elevated temperatures. McCoy (8) was the first one to do a systematic study of the hydrogen degradation effects of nickel, copper and iron at elevated temperatures. He concluded that hydrogen increases the creep rate of Ni and Cu because of the increase in dislocation mobility and density. The hydrogen embrittlement effects such as "hydrogen attack", and "hydrogen disease" may occur in carbide-strengthened Haynes 188 and NARloy-Z. Hydrogen attack has been observed in Co-based alloy (9, 10) and hydrogen disease has been observed in Cu (7). The present study focuses on the hydrogen effects on the creep properties of the alloys.

3. OBJECTIVES OF THE PROGRAM

The objectives of the program are a systematic study of the metallurgical, phenomenological, and mechanistic aspects of hydrogen effects in Haynes 188, Mo-50Re and NARloy-Z at high temperature. The goals of this program are to determine the effects on creep mechanisms of the above alloys as functions of alloy compositions and microstructures in the presence of low and high pressure hydrogen.

The scope of this program is outlined in the flow chart in Figure 1. The incremental stress creep rates and stress rupture lifetimes as influenced by external hydrogen pressures of 0.1-10 MPa (15-1500 psi) and temperatures from 400-1000°C, will be determined. The

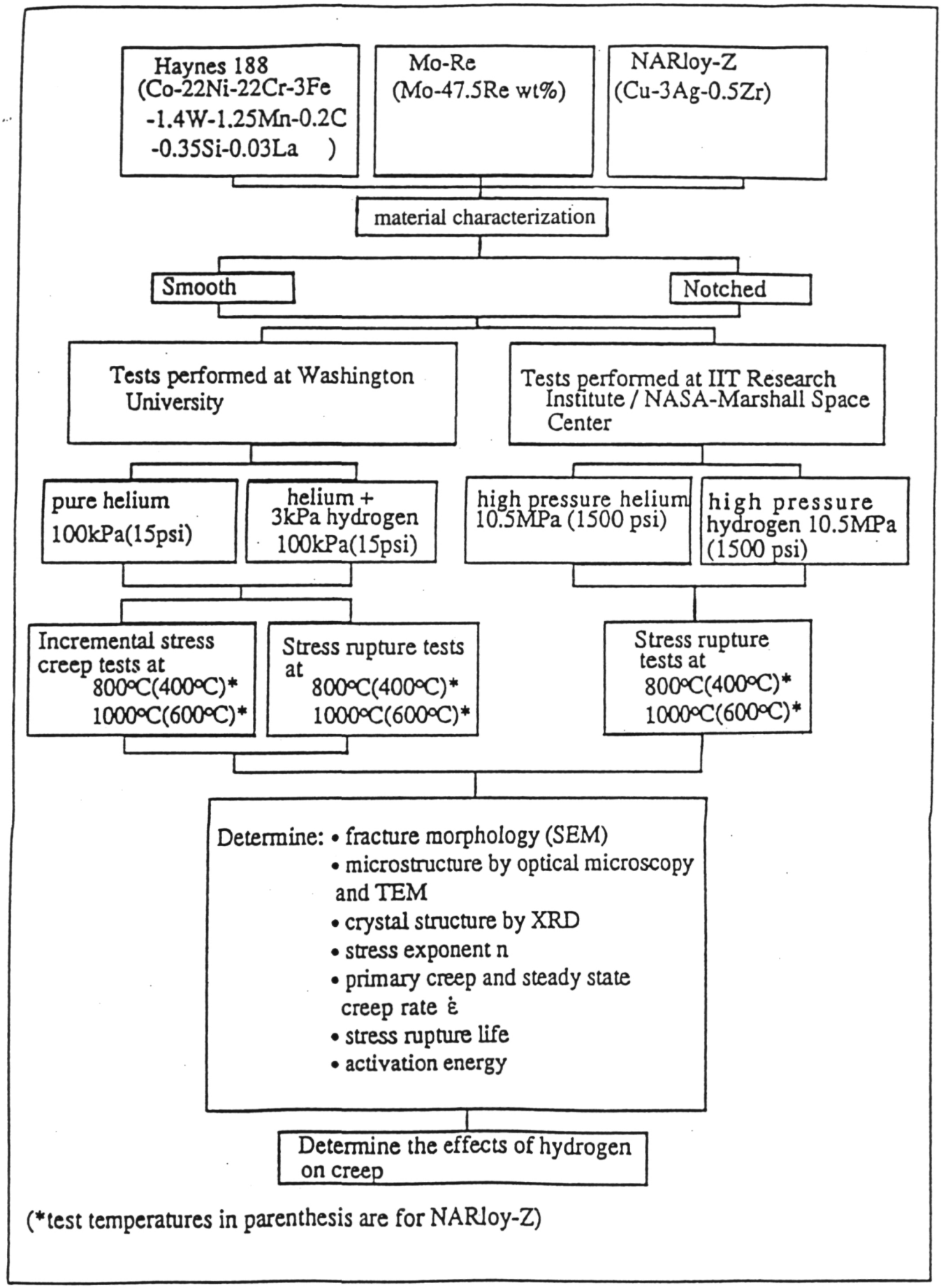

Figure 1: Flow chart showing scope of the program

effect of compositions, second phases, and grain size and shape will be correlated with hydrogen absorption and creep mechanisms. All possible approaches to imparting hydrogen resistance will be identified.

4. EXPERIMENTAL PROCEDURE

4.1. Material characterization

The Haynes 188 and Mo-Re have been procured and characterized by optical microscopy, X-ray diffraction (XRD) and transmission electron microscopy (TEM).

4.1.1 Haynes 188

Haynes 188 was procured from Haynes International (Kokomo, Ind.). The chemical composition of the alloy is shown in Table 1. The alloy is a solid solution strengthened cobalt-based alloy designed for sheet-metal components such as combustor and transition ducts in gas turbines for high temperature service in oxidation and sulfidation atmosphere. It is designed with the combination of strength characteristics of Haynes 25 and corrosion resistance of Hastelloy X. Tendency to form Laves phase is less in Haynes 188 than in Haynes 25 which results in ductility loss in the intermediate temperature range (11).

Cobalt has an allotropic transformation from low temperature HCP structure to FCC structure at 420°C. The high content of Ni in Haynes 188 strengthens the alloy by solid solution strengthening, and stabilizes austenite (γ) matrix to ambient temperatures as XRD pattern shown in Figure 2. Thus the possible deleterious effect due to repeated change in the crystal structures is eliminated. The formation of harmful hexagonal TCP Laves phase (Co_2W) that impairs both tensile ductility and impact strength due to intergranular fracture is reduced by utilizing solution annealing temperature of 1230°C. The Laves phase forms after prolonged exposure of $>$ 100 hours. Additions of silicon and iron are believed to have large effects on the formation of the Laves phase (12).

Table 1 Chemical composition of Haynes 188

Co	Ni	Cr	W	Fe	Mn	Si	C	La	B
Bal	20.0-	21.0-	13.0-	3.0*	1.25*	0.20-	0.05-	0.02-	0.015*
	24.0	23.0	15.0		—	0.50	0.15	0.12	

*Maximum.

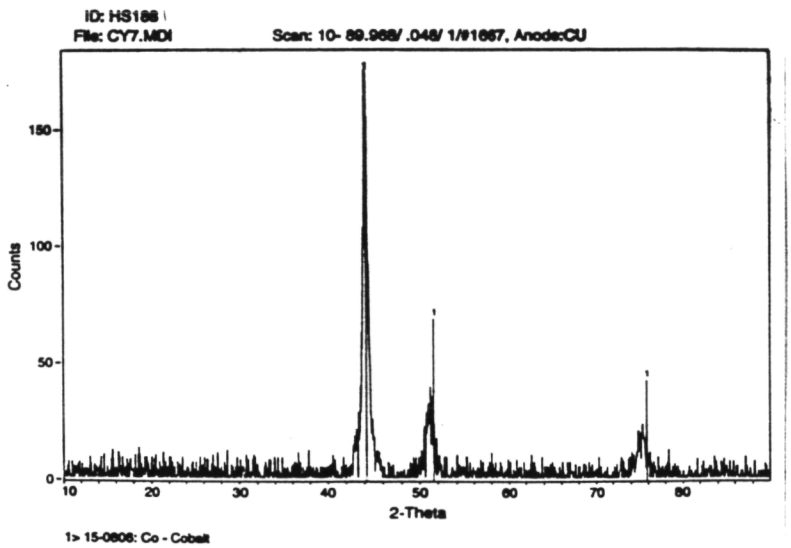

Figure 2: XRD pattern of Haynes 188

Haynes 188 is strengthened principally by the carbides (mainly $M_{23}C_6$ and M_6C). A high concentration of carbide forming elements such as Cr, W and Fe will determine carbide formation during aging. The typical solution annealing temperature is 1150-1200°C which renders all secondary carbides into solution The as received microstructures of Haynes 188 consists of extensive carbides (M_6C) along the grain boundaries as shown in Figure 3. The secondary carbides ($M_{23}C_6$) start to precipitate within the matrix and grain boundaries when the alloy is heated to 600°C. Those secondary carbides go back in solution when temperature exceeds 1100°C. The major function of solution annealing is to recrystallize the structure to develop the required grain size and morphology. However, grain growth is very fast at this temperature because of the absence of carbides. In order to take advantage of the fine grain size, time and temperature must be controlled to achieve optimum grain size as well as carbide solutioning and precipitation.

Haynes 188 possesses relatively low stacking fault energy and therefore cross-slip could be difficult. Low stacking fault energy provides high temperature creep resistance and high work hardening exponent for Haynes 188 (13). The yield stress and hardness increase rapidly with increasing cold deformation as shown in Figure 4. Haynes 188 shows high work-hardening exponent of 0.70 (13). Therefore, high resistance to necking is expected. For materials with high work hardening exponent, numerous cold rolling passes with subsequent intermediate annealing is required to get large deformation.

4.1.2 Mo-47.5Re

Mo-Re with chemical composition of Mo-47.5 Wt. % Re procured from H. Cross Company (Weehawken, NJ) was manufactured by powder metallurgy method: sintered, cold rolled and annealed at 1800°C then normalized to room temperature in hydrogen atmosphere. It was developed for improving ambient temperature ductility and high temperature strength of Mo. Mo has a ductile-brittle transition temperature (DBTT) at

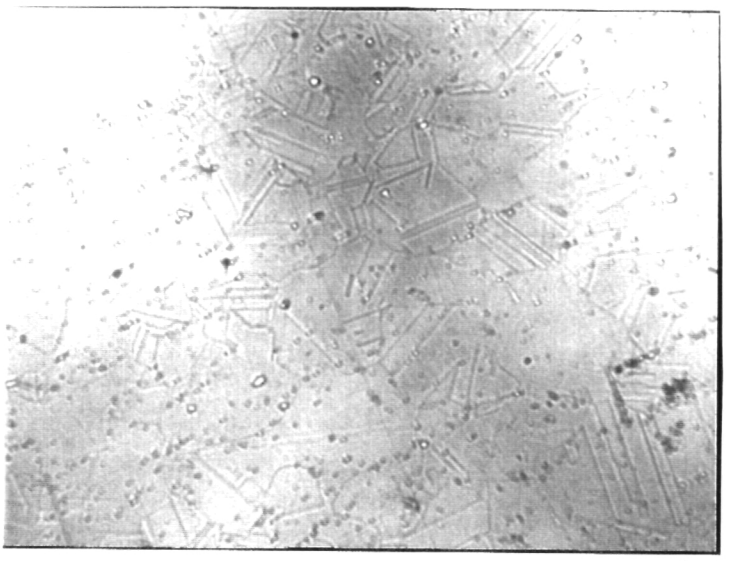

(a) X200

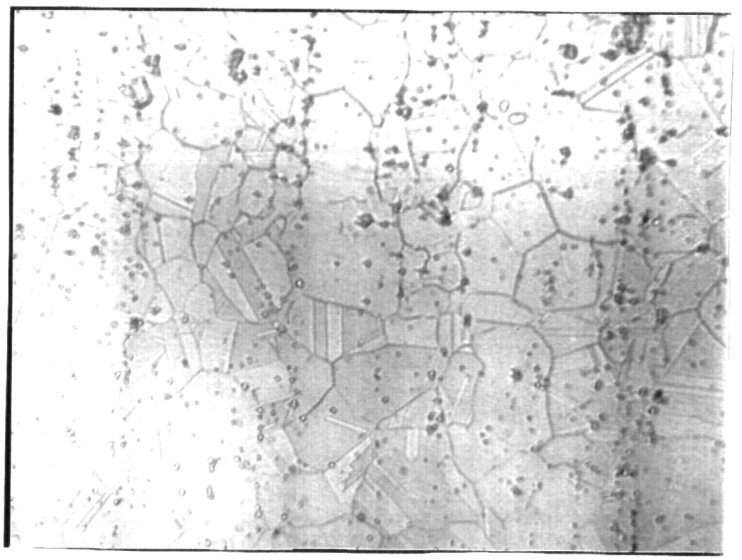

(b) X200

Figure 3: Optical microstructures of Haynes 188 (a) Transverse (b) Longitudinal

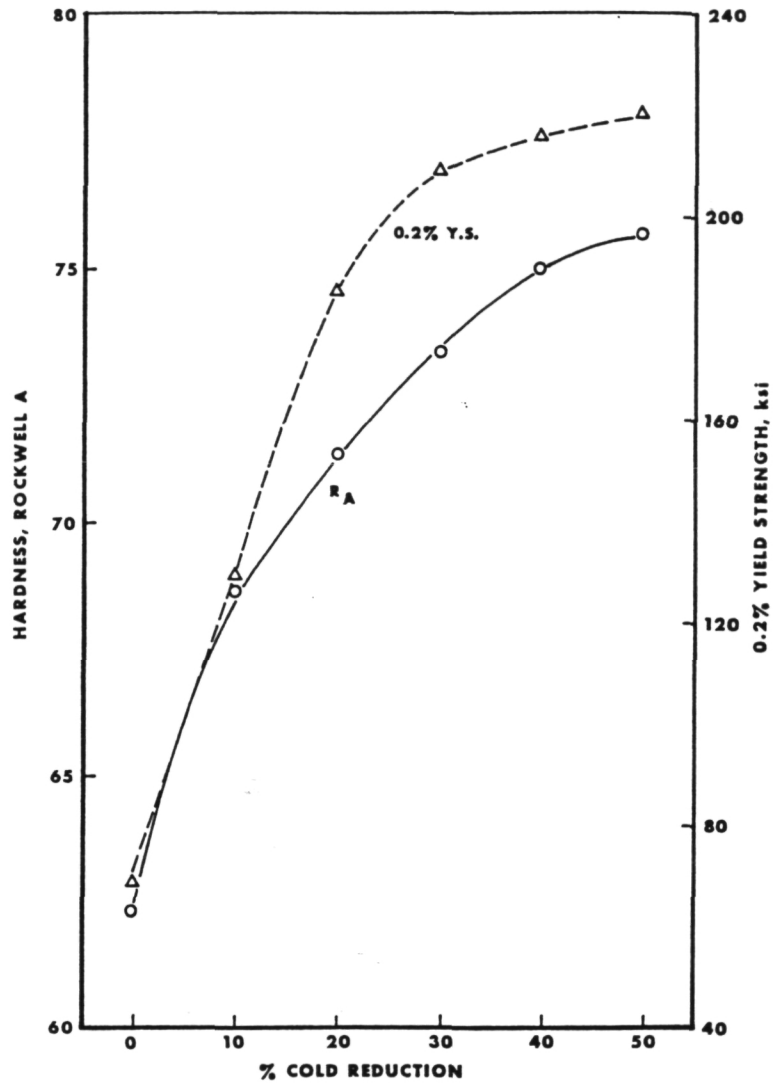

Figure 4: Effect of cold rolling on the hardness and yield strength of Haynes 188

room temperature which severely limits its applications. The addition of Re to Mo increases the high temperature strength and low temperature ductility.

The most common Mo-Re alloys contain about 5, 41, and 50 % Re (actually 47.5%). The 5 and 41% alloys are used for thermocouples and structural applications in aerospace industry. The 50% alloy is typically specified for high temperature structural components and has received considerable amount of interest in the NASP program because of its good high temperature strength and low temperature ductility typically specified for high temperature structural components.

Mo-50Re is a two phase alloy with predominately BCC solid solution as shown in phase diagram in Figure 5 and XRD pattern in Figure 6 and a small amount of χ phase which is a BCC phase isomorphous with α-manganese found in some complex iron-based alloys (14). When the temperature is raised up to 1150°C most χ phase transforms into hard and brittle σ phase (15) which has a tetragonal (D_{2h}^{14}) crystal structure isomorphous with the σ phase found in iron-chromium alloys.

The high solubility of Re in Mo is not unexpected due to their similar atomic diameter (Re:2.740Å and Mo:2.725Å). Mo-Re has a stacking fault energy lower than that of commercial grade Mo (16). The stacking fault energy of Mo falls proportionally as the Re content increases, and hinders the cross-slip of dislocations. The stacking fault energy of Mo is approximately 450 erg/cm^2, compared to 350 erg/cm^2 of Mo-Re.

Mo-50Re can be fabricated by either warm or cold working. Unlike Mo which has a DBTT just above room temperature, Mo-50Re fractures in a ductile manner at temperatures as low as 77K. The excellent ductility of Mo-50Re results from the promotion of extensive deformation twinning as a primary mode of deformation (17). It can be rolled into sheet with high reduction ratio (90%) at room temperature without intermediate annealing. Microstructures of cold rolled alloy are shown in Figure 7.

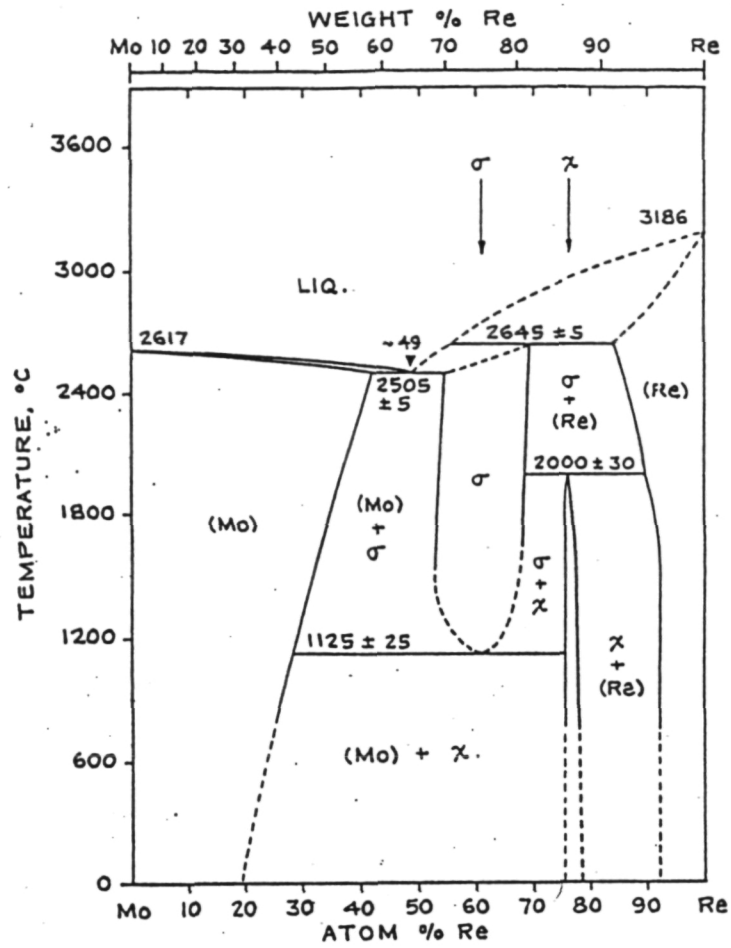

Figure 5: Phase diagram of Mo-Re

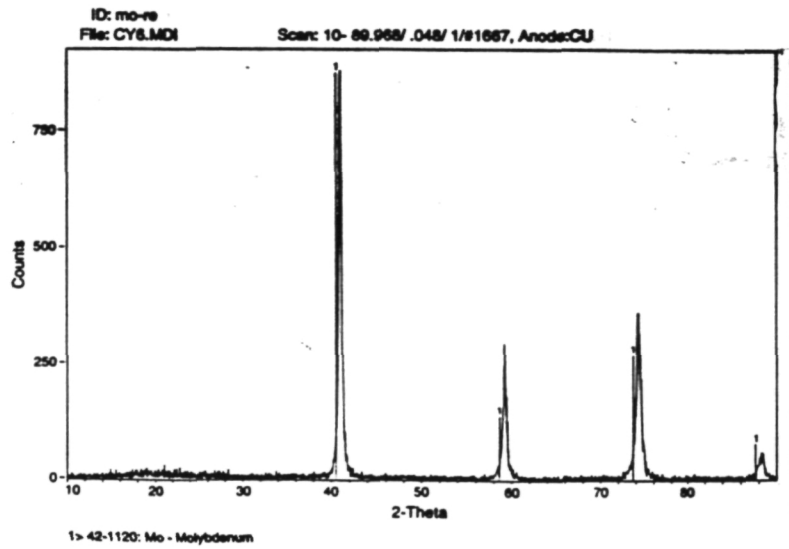

Figure 6: XRD pattern of Mo-Re

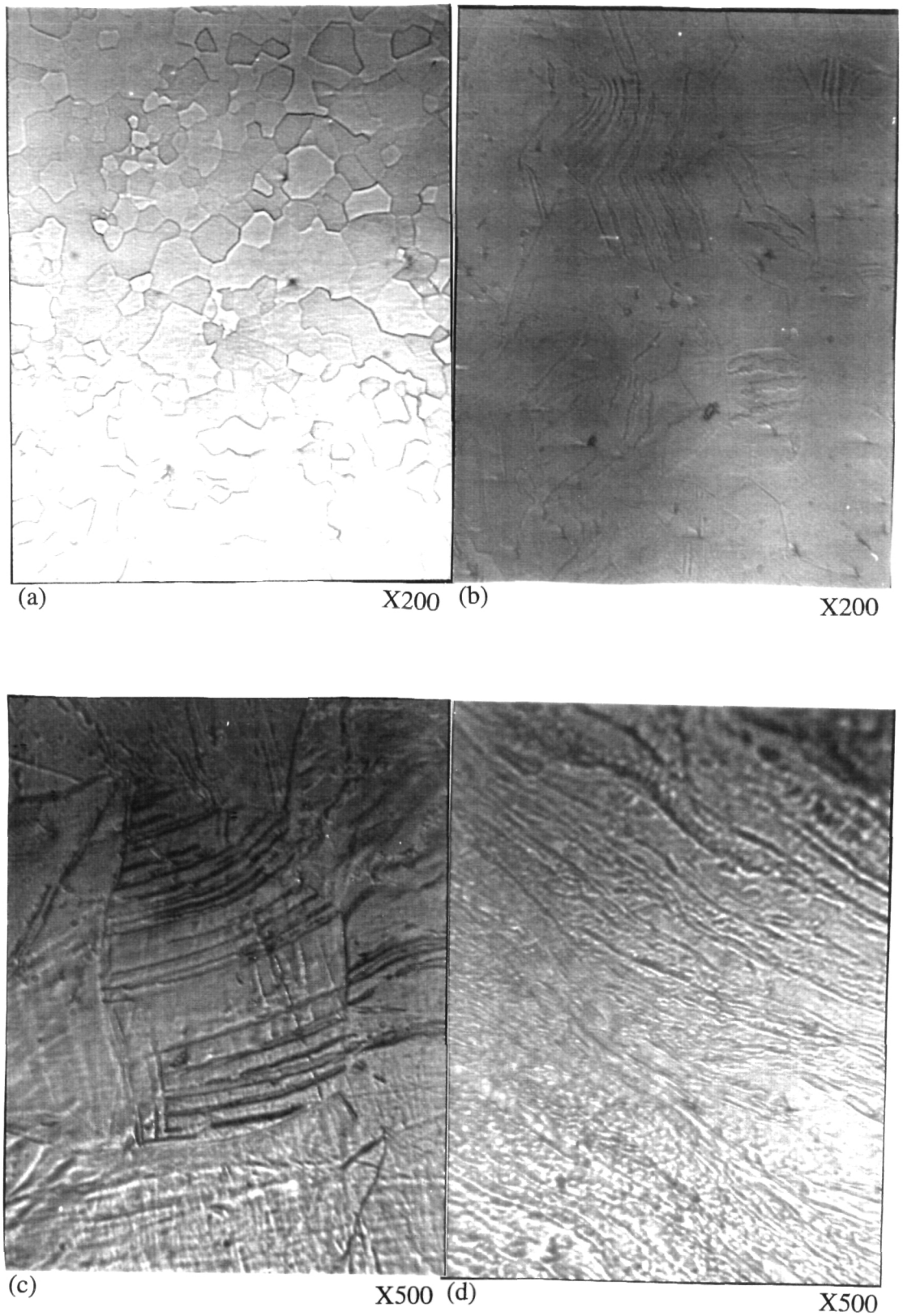

Figure 7: Microstructures of Cold rolled Mo-Re (a) as received (b) 50% (c) 75% (d) 90%

4.2. Creep testing

Incremental stress and constant stress rupture tests are the principal methods used in the present study for determining the mechanical behavior in hydrogen atmosphere at elevated temperatures. The low pressure hydrogen (5% hydrogen + argon) tests are performed at Washington University and tests in high pressure (1500 psig) hydrogen atmosphere are performed at IIT Research Institute / NASA - Marshall Space Flight Center, Alabama.

4.2.1 Experimental set-up for creep testing in low pressure hydrogen atmosphere

The set-up (Figure 8) consists of testing chamber which is hermetically vacuum-sealed for atmosphere control. Tungsten is used as heating element, and molybdenum foil is used as thermal shield. Specimens are gripped in water-cooled TZM pull rods and an extensometer attached to the specimen is used for elongation measurement as shown in Figure 8. The chamber can be used for creep testing at temperature up to 1100°C with 10^{-6} Torr degree of vacuum at both ambient and high temperatures. The chamber is mounted on an ATS creep frame as shown in Figure 9. The extensometer is connected to LVDT (made by ATC with model # 6234A05B01) by a cross linkage with a reduction ratio of 2:1. The LVDT is calibrated by attaching a microdialmeter on pull rods to measure the elongation of specimens. The LVDT voltage output is converted to strain by Universal Scanner 4280 with LVDT card. The data are collected by data acquisition system in Hewlett-Packard 86 computer.

Samples of Mo-Re and Haynes 188 were machined with gauge length of 0.75 inch and diameter of 0.125 inch as shown in Figure 10. All samples were ground with 1000 mesh emery paper to remove surface oxide layer before loading into pull rods. The testing chamber was first evacuated to 10^{-6} Torr and then slowly heated to testing temperature. The rise of temperature was slow and the chamber was always kept at the degree of vacuum of 10^{-5} Torr level during heating. The desired gas of pure argon gas or argon +

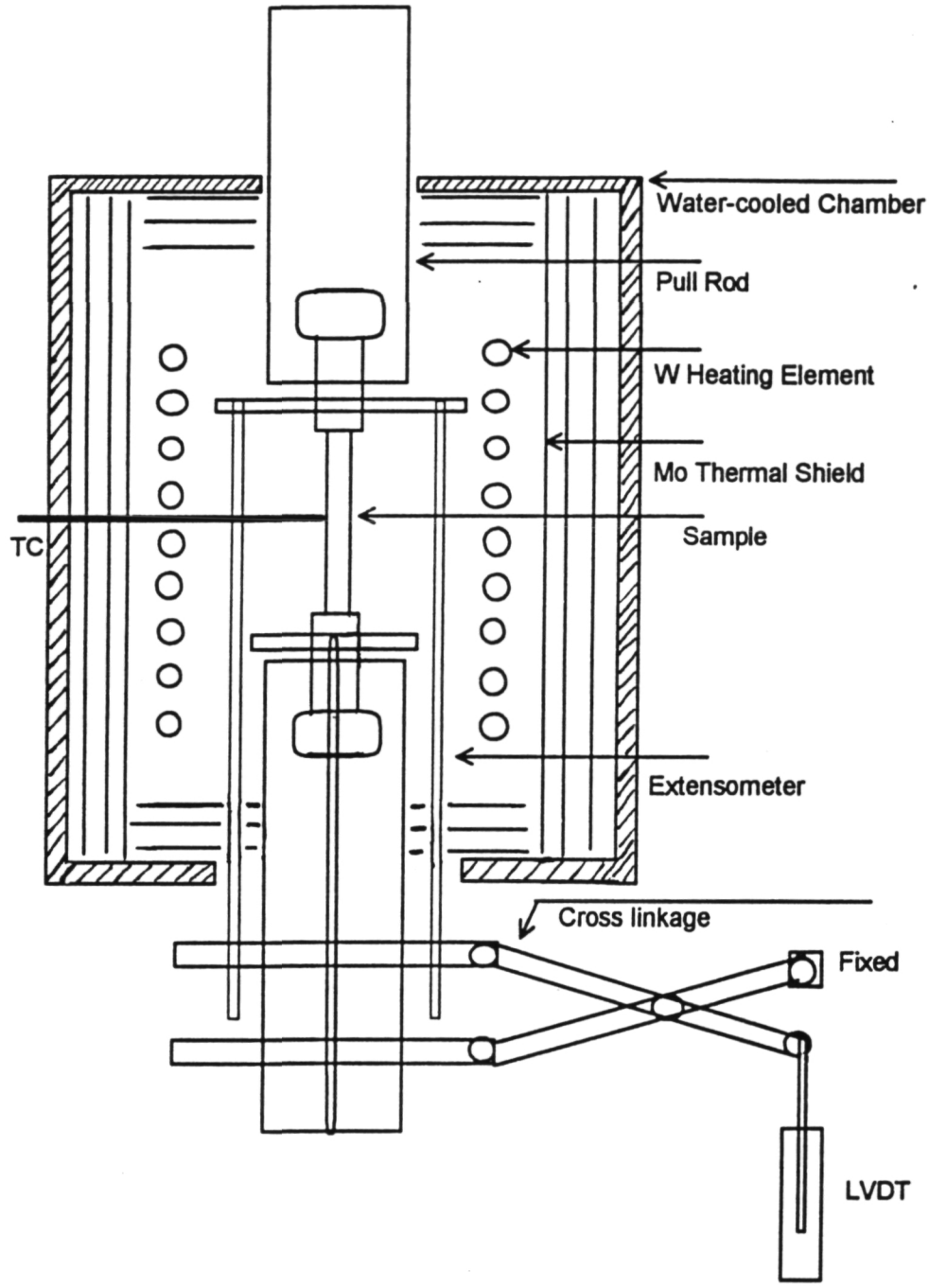

Figure 8: Testing assembly inside chamber

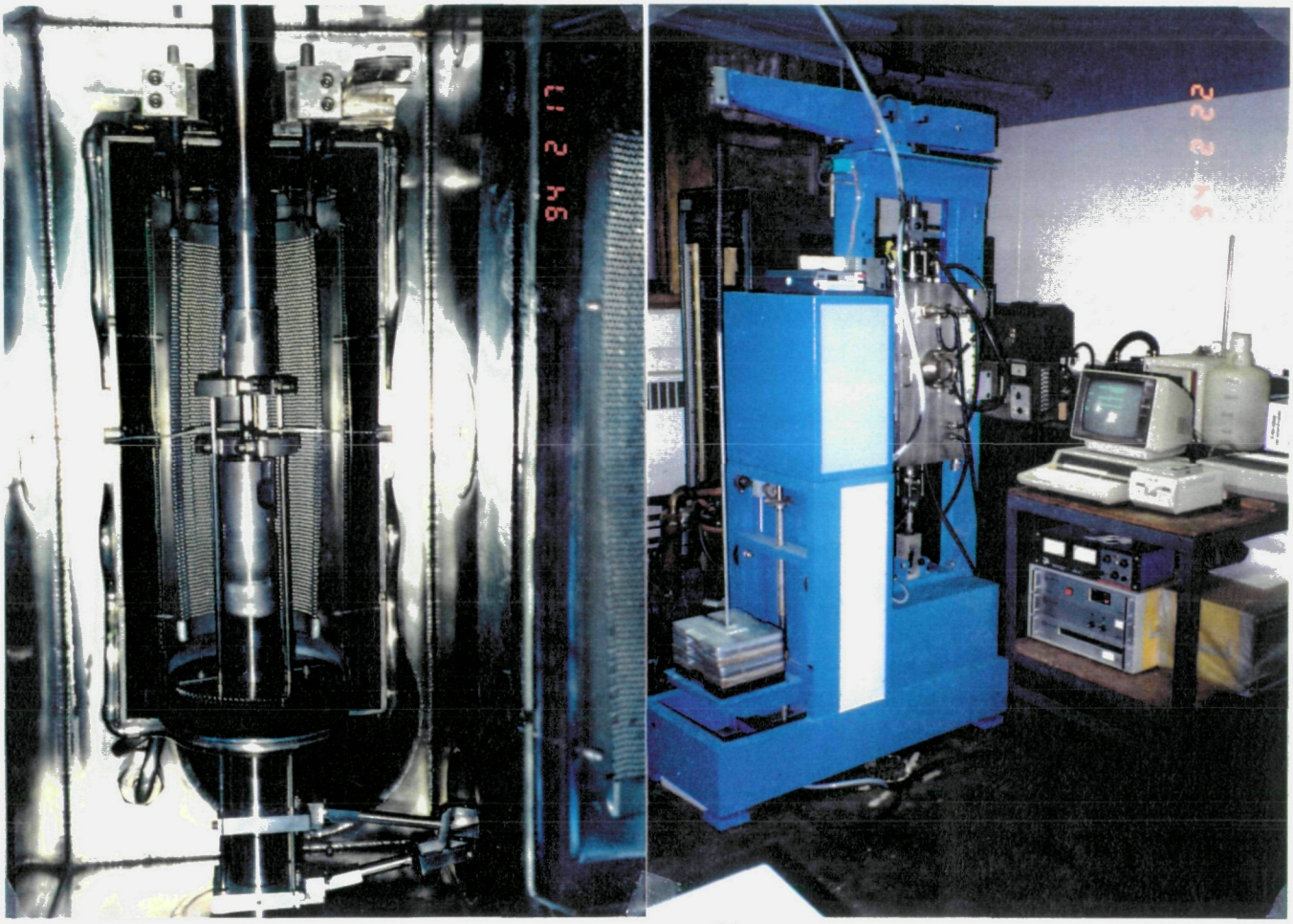

(a) (b)

Figure 9: (a) Chamber and (b) Creep frame

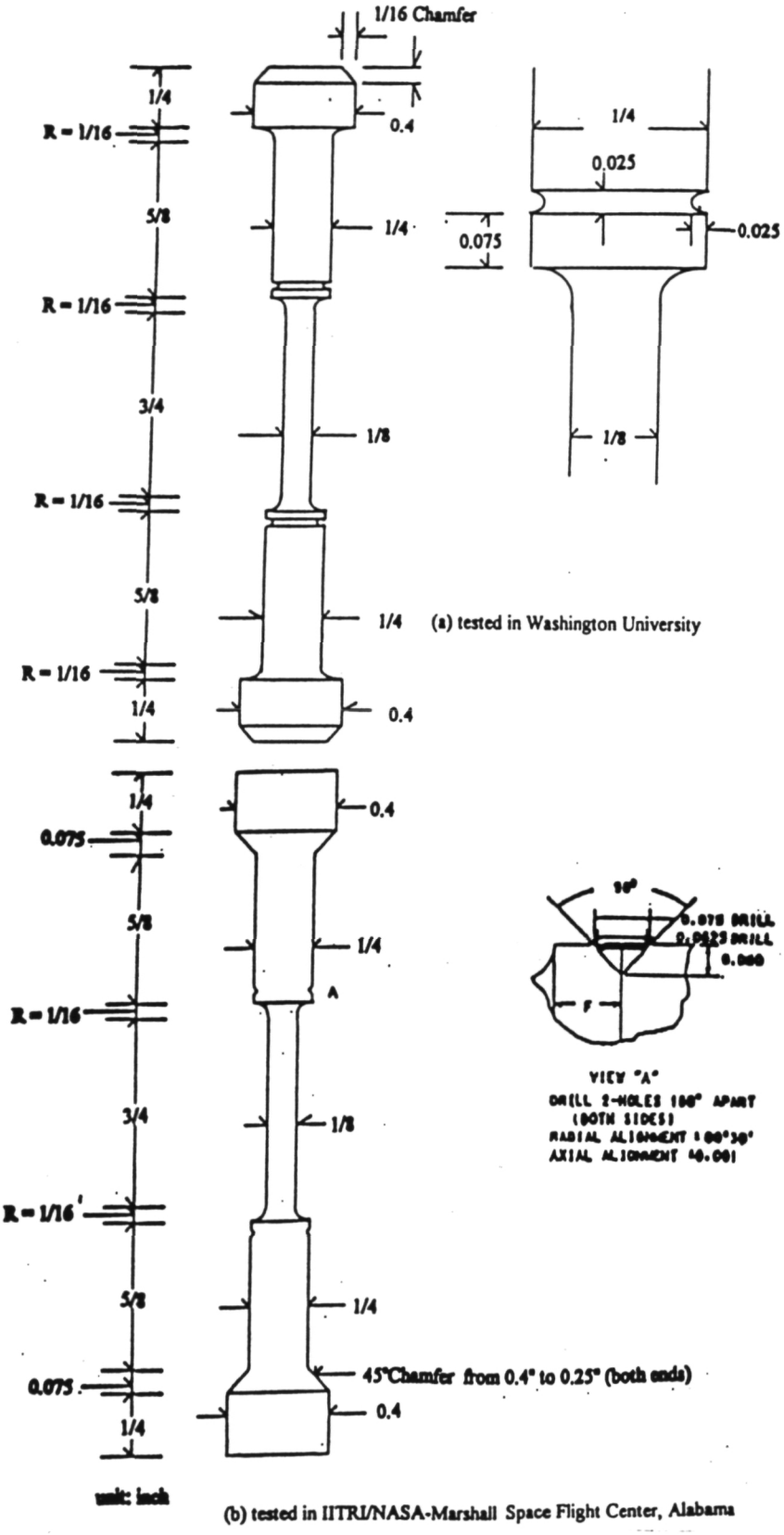

Figure 10: Sample geometry (a) tested in Washington University, (b) tested in IITRI/NASA-Marshall Space Flight Center

Hydrogen mixture gas with purity of 99.999 % is introduced when the desired temperature is reached. The chamber pressure is controlled 1 psi larger than atmosphere pressure to prevent air entry into the chamber. Each applied stress level lasts for 24 hr then stress is increased to a higher value. The sample elongation is measured by LVDT and recorded by data acquisition system and computer.

4.2.2 High pressure hydrogen facility at NASA-Marshall Space Flight Center

The high pressure tests are performed at Hydrogen Test Facility (HTF) at NASA-Marshall Space Flight Center. The high temperature and high pressure hydrogen test system were designed and built by Pratt and Whitney and can operate at temperatures up to 1800°F (982°C) and pressure up to 10 ksig (69 MPa). The specimen elongation is measured by LVDT and recorded by chart recorder. Hydrogen used for testing is chosen according to MIL-P-27201B, the propellant grade specification. This specification limits total impurities to less than 50 ppm, and in particular the oxygen limit is less than 1 ppm.

Work at HTF uses a purge sequence that assures propellant grade standard. The purge sequence is as follows :

1. Install specimen in vessel and seal system
2. Evacuate pressure vessel to less than 1 Torr
3. Pressurize systems to 500 psig with gas nitrogen (3.4 MPa)
4. Vent system down to 10 psig (68 kPa)
5. Evacuate vessel to less than 1 Torr
6. Repeat steps 3, 4 and 5, four additional times
7. Pressurize system to 500 psig (3.4 MPa) with the test gas
8. Vent system down to 10 psig (68 kPa)
9. Repeat steps 7 and 8, four additional times
10. Fill vessel with test gas
11. Perform test

12. Vent test gas out

13. If test gas was hydrogen, fill vessel to 500 psig nitrogen.

14. Vent vessel to 10 psig (68 kPa)

15. Repeat steps 13 and 14 four additional times

16. Vent out all gas in the chamber

17. Open system

4.3 Creep test results

The incremental stress creep tests have been performed at 800°C for Mo-Re and Haynes 188 in both pure argon and hydrogen-containing atmospheres. After creep testing the strain rates at each stress level are calculated after the compensation of cross section area reduction caused by elongation of samples. The stress exponents were calculated to evaluate the deformation mechanisms.

Hydrogen has no effect on the creep rate of Haynes 188 as shown in Figure 11; however, creep rate seems to be slightly higher for Mo-Re in hydrogen-containing atmosphere as shown in Figure 12. Haynes 188 tested in both atmospheres has the same reduction of area (RA) of 77 % and Mo-Re has a RA of 90% in both atmospheres. Stress exponents of around 4 for Haynes 188 in both atmospheres are observed which indicate the deformation mechanism to be dislocation climb. Stress exponents of 8 to 9 for Mo-Re are observed which are indicative of power law breakdown region with dislocation glide controlled deformation mechanism.

4.4 Microstructures of the tested materials

4.4.1 Haynes 188

The optical microstructures of Haynes 188 tested at 800°C in both atmospheres shown in Figure 13 reveal extensive secondary carbide ($M_{23}C_6$) formation within grain boundaries. Hydrogen did not cause significant differences in both deformed and undeformed (grip section) part of the sample.

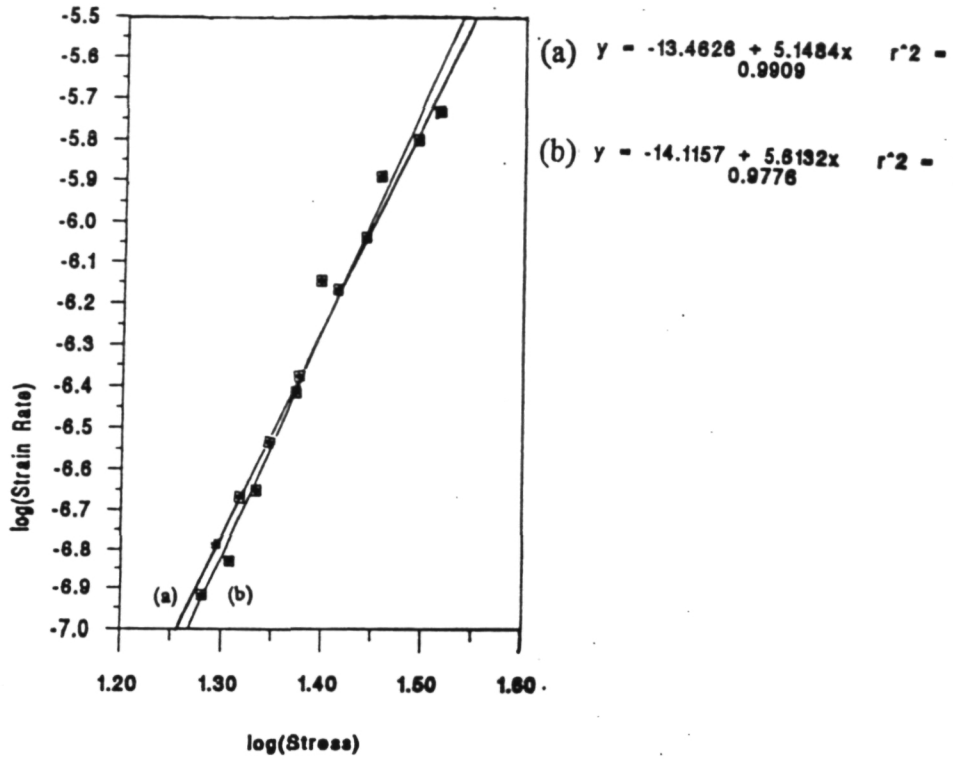

Figure 11: Stress exponent of Haynes 188 at 800°C in (a) argon (b) hydrogen-containing atmosphere

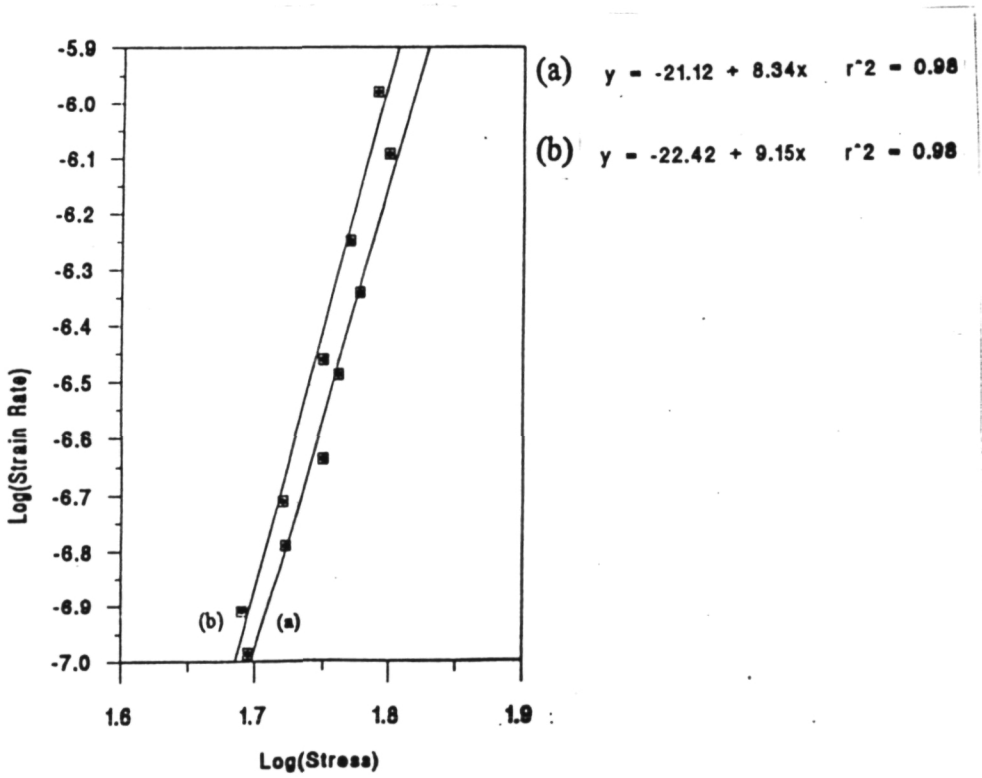

Figure 12: Stress exponent of Mo-Re at 800°C in (a) argon (b) hydrogen-containing atmosphere

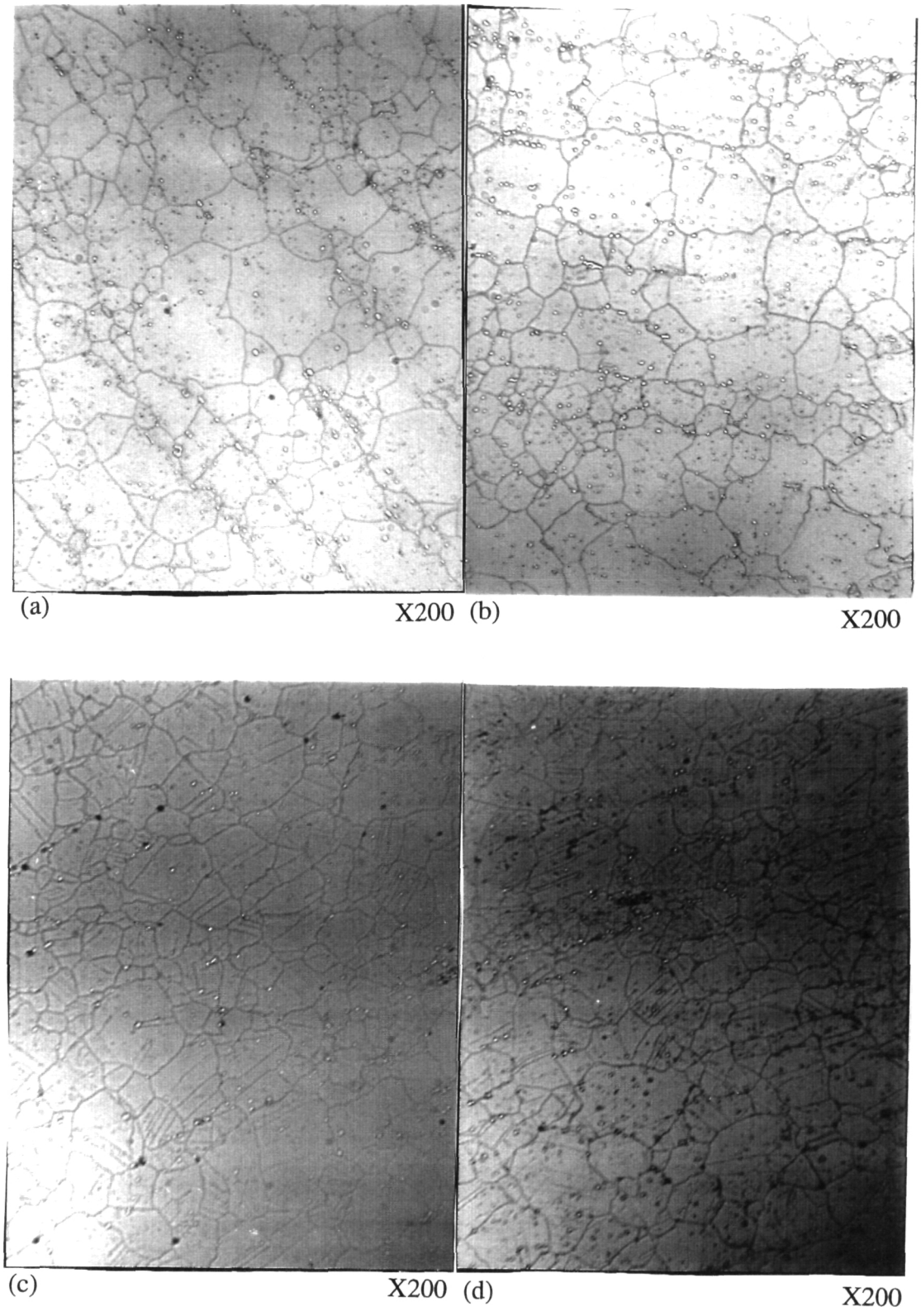

Figure 13: Optical microstructures of Haynes 188 tested in (a)Ar, undeformed (b) Ar + 5% H_2, undeformed (c) Ar, deformed (d) Ar + 5% H_2, deformed

Fracture surface of Haynes 188 crept to failure at 800°C in Argon and hydrogen-containing atmospheres shown in Figure 14 are similar. Fracture was caused by void coalescence, and the fracture surface were rough and dimpled on a very fine scale. This may reflect the fine carbide dispersion present in this alloy.

(i) Undeformed region exposed to low pressure hydrogen: TEM image of a specimen cut at the grip section (and therefore undeformed, but exposed and annealed at high temperature and atmosphere) from sample crept at 800°C in H_2 are shown in Figure 15. Widely dispersed, spheroidal particles, 1-5μm in diameter were identified as $D8_4$ (M_6C) type carbide which are also observed under optical microscopy. The specimen also contained a dense distribution of small Cr-rich carbides frequently found at grain boundaries. These carbides are 200-500 nm in diameter and are often faceted and aligned. Those small secondary carbides are not present in the as received Haynes 188. That is because the as received Haynes 188 is solution annealed at 1150°C thus all secondary carbides go into solution.

(ii) Deformed region exposed to low pressure hydrogen: The deformed microstructures of Haynes 188 crept at 800°C in H_2 atmosphere is shown in Figure 16. The material is densely filled with dislocations as shown in Figure 16(a) and the grains contain elongated roughly aligned subgrain boundaries formed by the unidirectional creep test stress. Frequently, the secondary carbides which formed during the creep test align with these subgrains as seen in Figure 16(a). Microtwinning was frequently observed as shown in Figure 16(b). A large number of sessile edge 1/2<110> type of dislocation are present (the horizontal, parallel lines in Figure 16(c), although the majority of dislocations are of mixed type in complex tangles. Dislocation loops as shown in Figure 16(d) and extended faults were also observed.

(iii) Undeformed region exposed to argon: Figures 17a-17d are transmission electron micrographs of an undeformed section of Haynes 188 crept at 800°C in Ar. The structure

is essentially the same as that seen in sample exposed in H_2. Within grains the carbides have clearly formed on {111} slip planes as shown in Figure 17(a, b). Within {111} twin boundaries, secondary carbides were aligned with the interface plane as shown in Figure 17(c), and this {111}alignment appears to also carry through to non-{111}, incoherent twin boundaries as shown in Figure 17(d).

(iv) Deformed region exposed to argon: Haynes 188 crept at 800°C in Ar is shown in Figure 18. Similar to the microstructures of material crept in H_2, a high density of dislocations is present, and elongated subgrain have formed as shown in Figure 18(a, b). Many bent microtwins are present, and grain and subgrain boundaries are heavily decorated with secondary carbides. Dislocations are tangled, mixed b=1/2<110> type, with many dislocation loops present as shown in Figure 18(c). Small carbide nuclei can be seen at very high magnification as shown in Figure 18(d).

4.4.2 Mo-Re

The optical microstructures of Mo-Re tested at 800°C in both atmospheres shown in Fig. 19 indicate no significant differences in deformed and undeformed part of the sample.

STEM was used in backscattered scanning mode to get high resolution image of the fracture surface of specimen crept at 800°C in Ar and H_2 atmospheres. Specimen crept in Ar and H_2 have similar ductile fracture surfaces, displaying a void coalescence failure mode as shown in Figure 20.

5. DISCUSSION

I. Haynes 188

The Haynes 188 tested in 5% hydrogen + argon did not exhibit any degradation effect with respect to that tested in pure argon and both have stress exponents around 4 which indicate the deformation mechanism to be dislocation climb. However, degradation of Co-based alloys has been observed previously in hydrogen atmosphere (9, 10). This probably can be explained as follows:

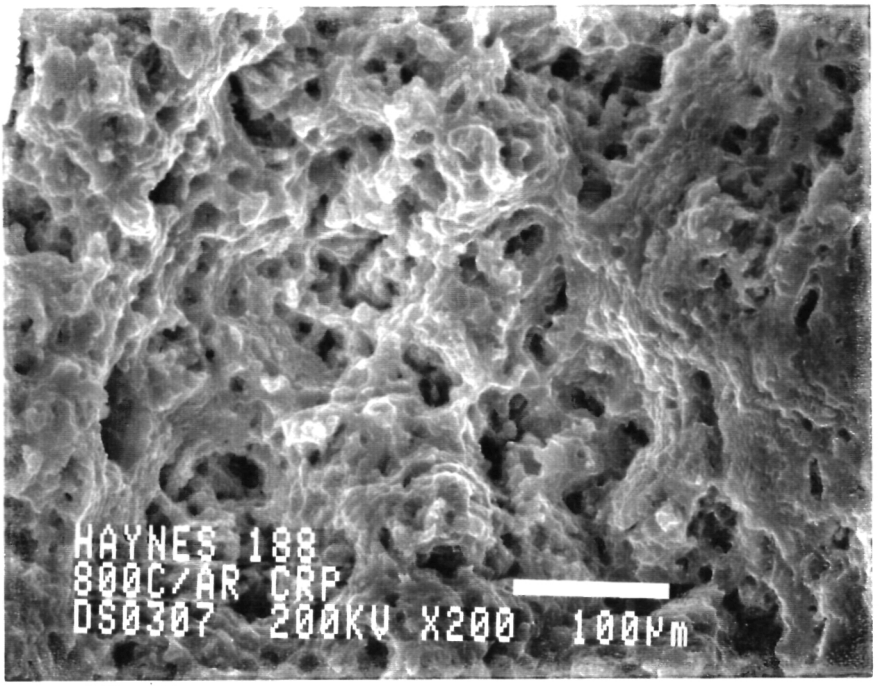

(a)

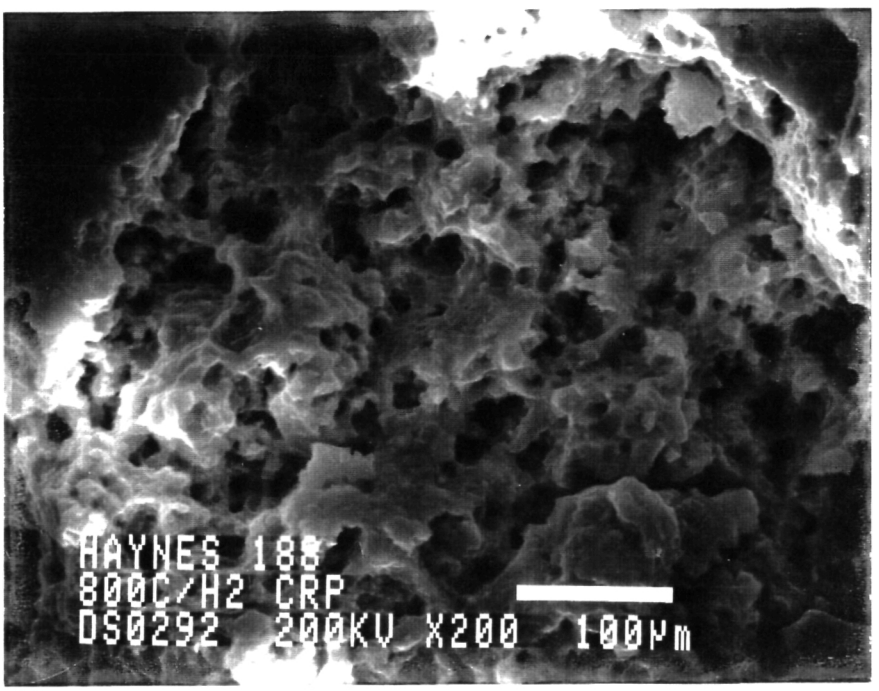

(b)

Figure 14: Fracture surface of Haynes 188 (a) argon atmosphere (b)H_2 atmosphere

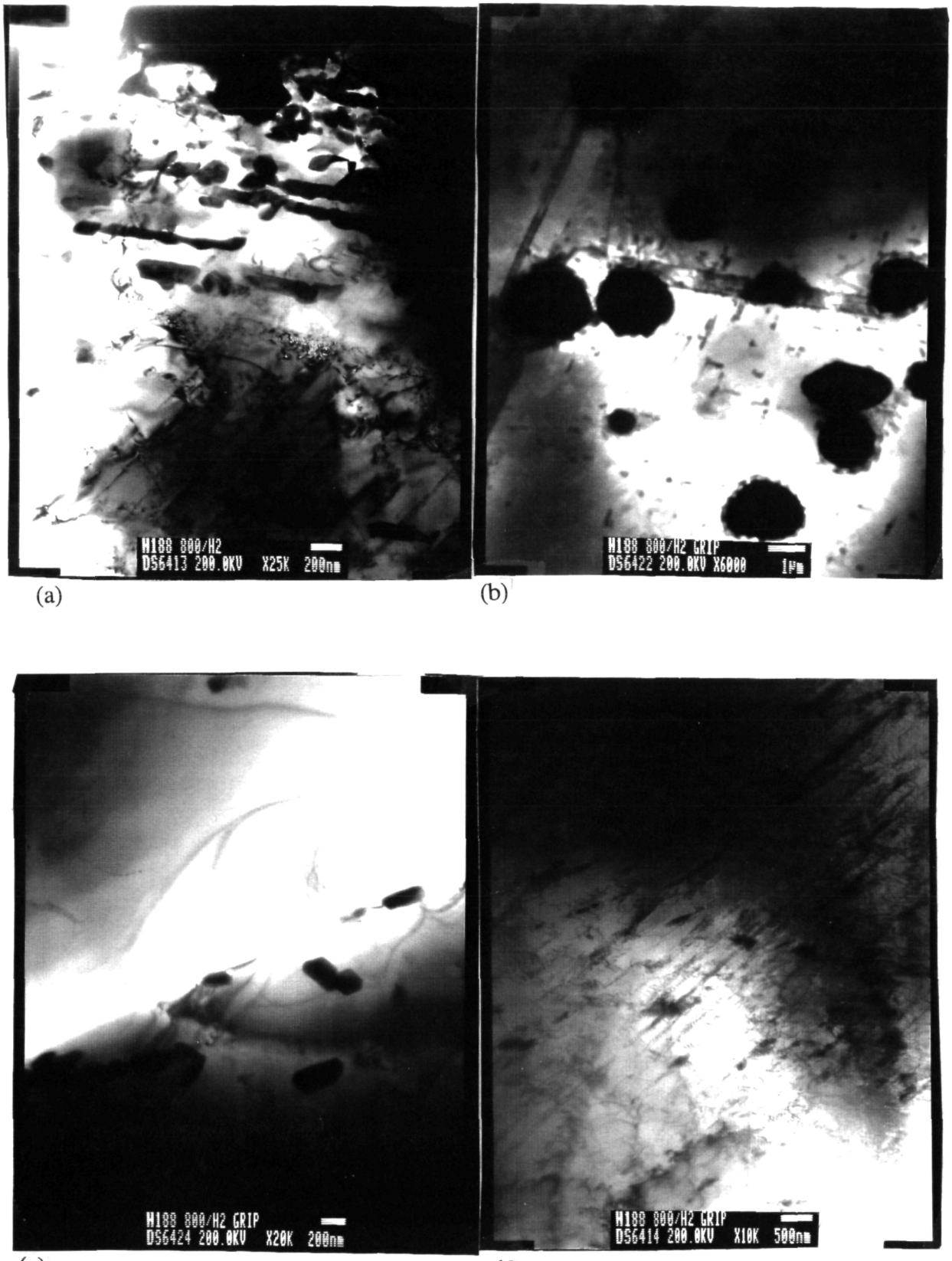

(a) (b)

(c) (d)

Figure 15: TEM observation of Haynes 188 tested in H_2 atmosphere and undeformed

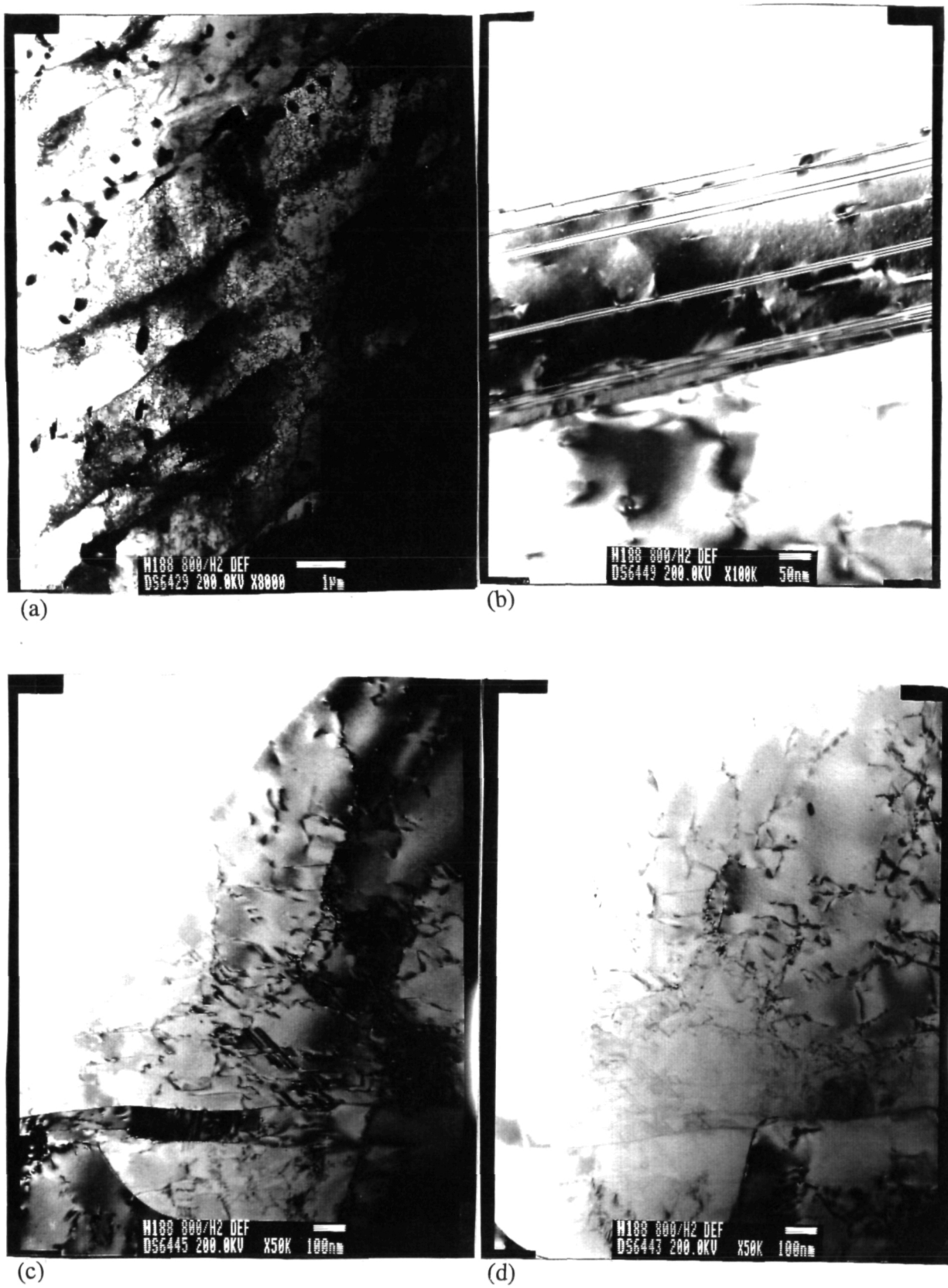

(a) (b)

(c) (d)

Figure 16: TEM observation of Haynes 188 tested in H_2 atmosphere and deformed

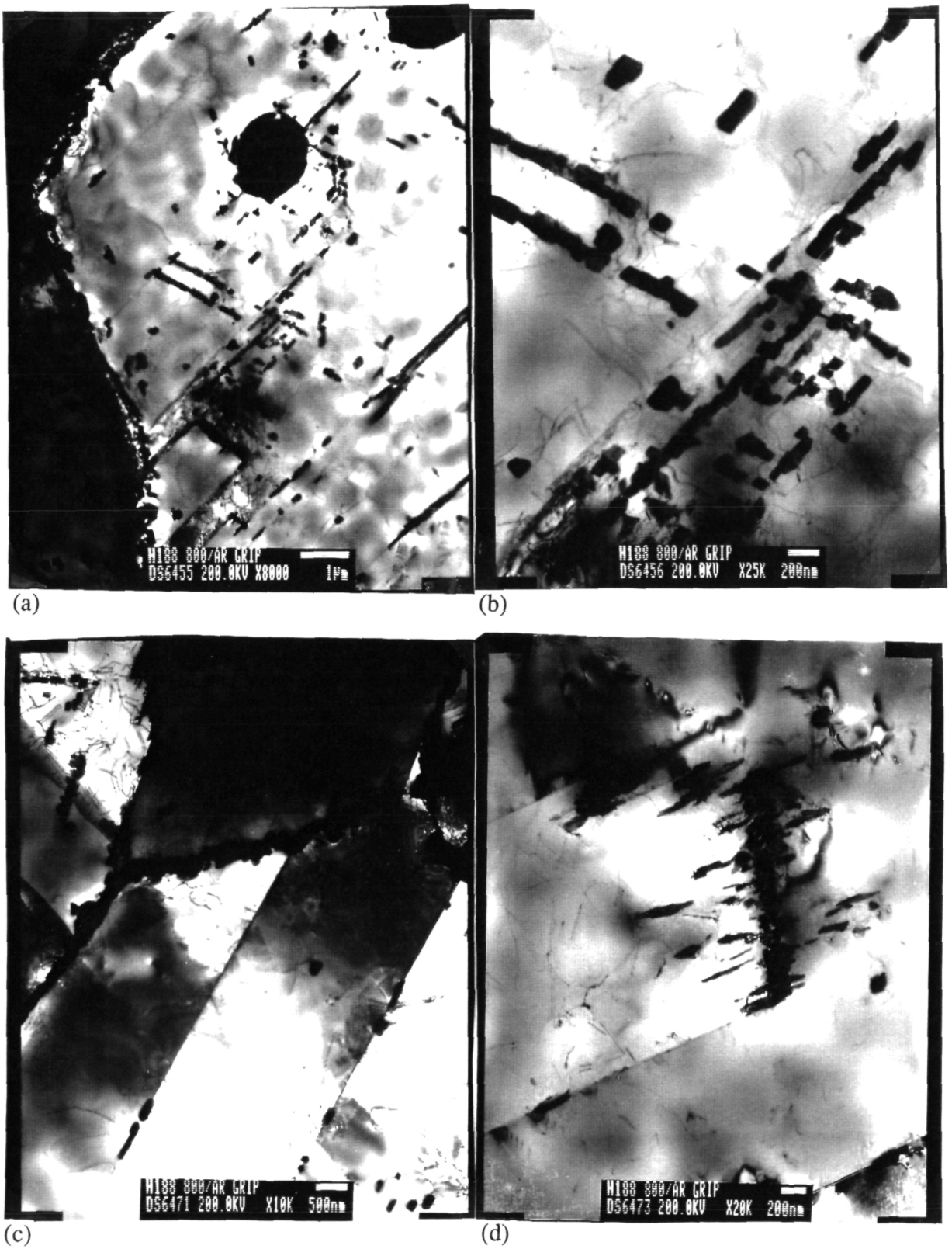

Figure 17: TEM observation of Haynes 188 tested in argon atmosphere and undeformed

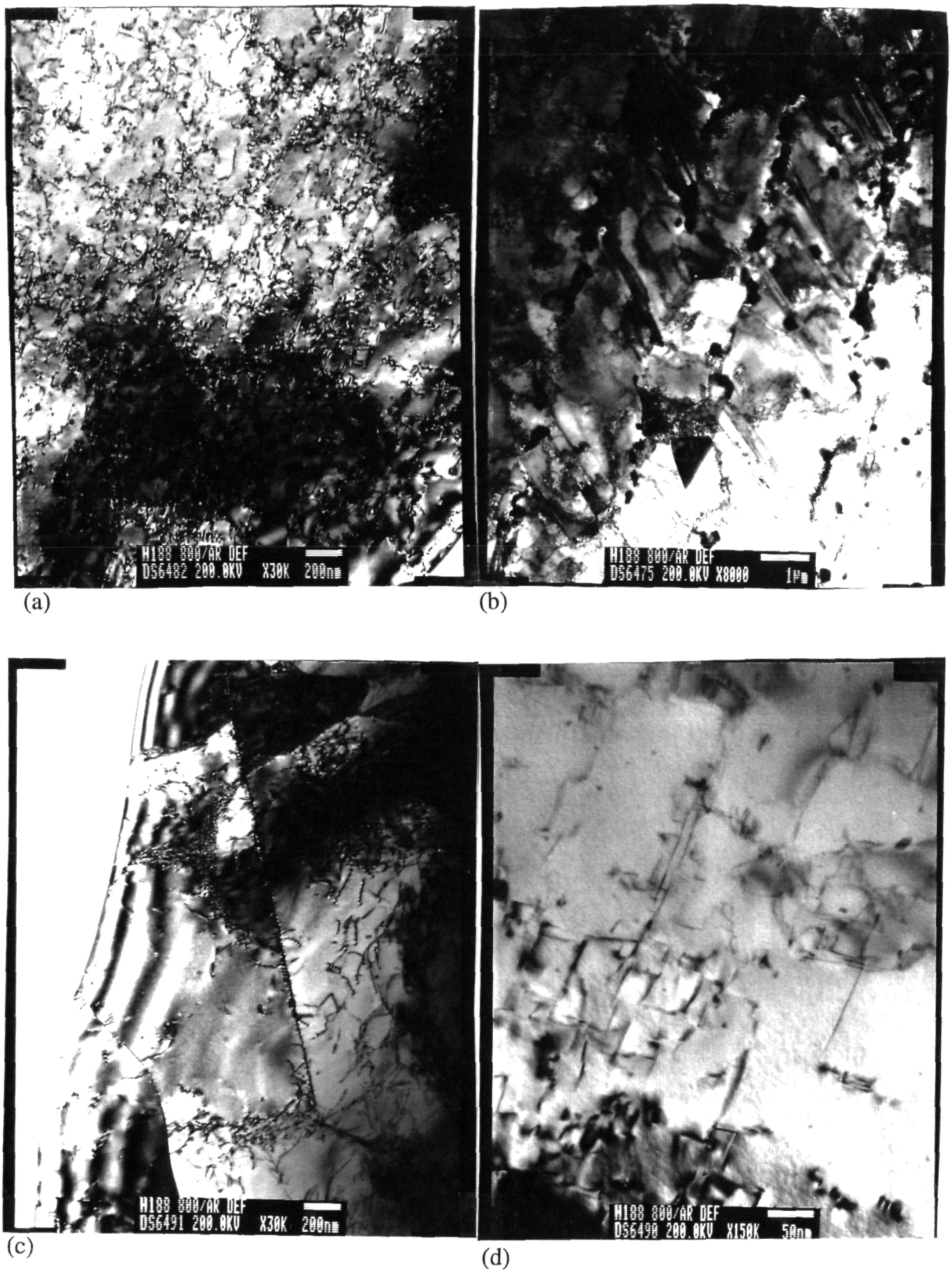

Figure 18: TEM observation of Haynes 188 tested in argon atmosphere and deformed

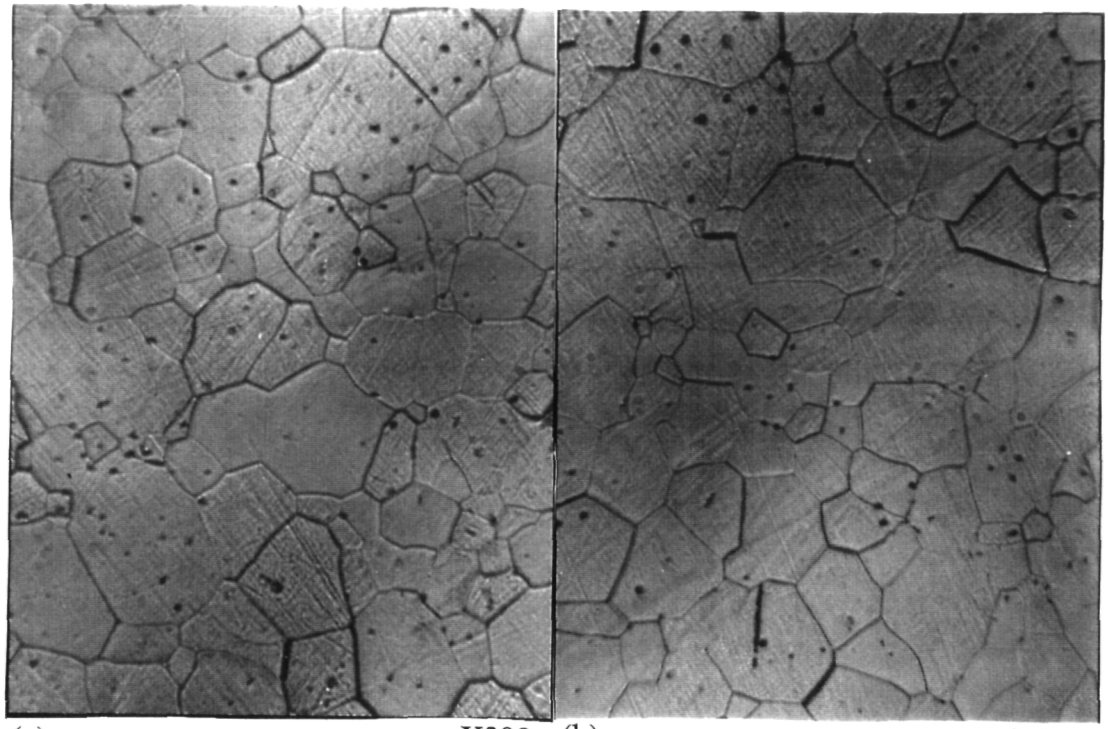

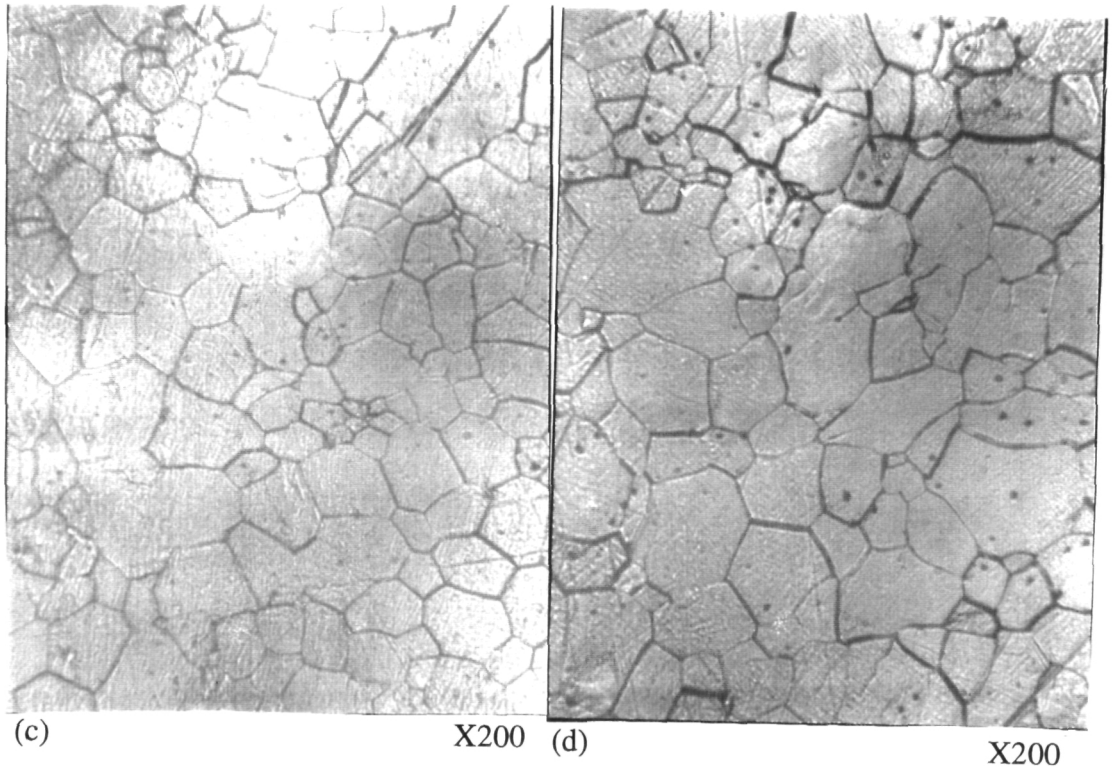

Figure 19: Optical microstructures of tested Mo-Re (a) argon, undeformed (b) H_2, undeformed (c) argon, deformed (d) H_2, deformed

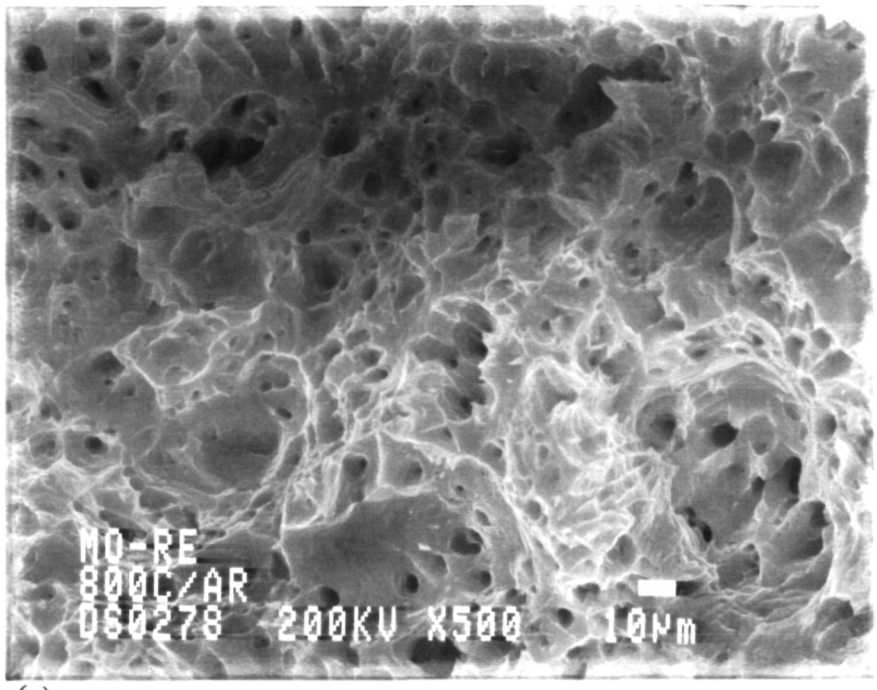

(a)

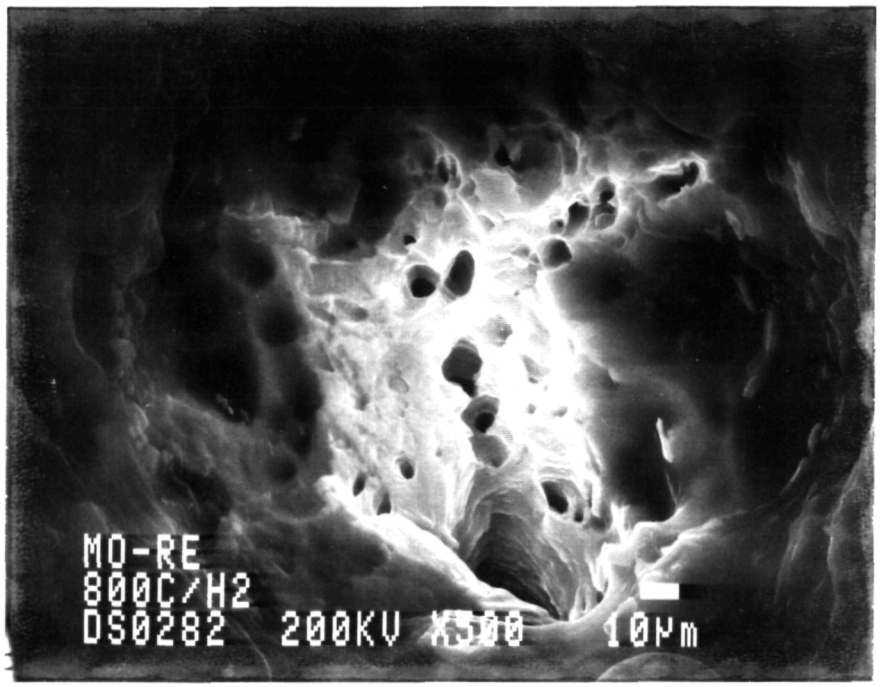

(b)

Figure 20: Fracture surface Mo-Re (a) argon atmosphere (b) H_2 atmosphere

According to Sievert's law (18):

$$S = K\sqrt{p}$$

5% hydrogen causes the reduction of hydrogen solubility to be 22% compared with pure hydrogen in references. Therefore 5% hydrogen does not cause appreciable degradation effects in Haynes 188.

The hydrogen degradation effects in Co-based alloys referred previously have compositions:

S-816-----43Co-20Ni-20Cr-4W-3Mo-4Fe-0.4C tested at 815°C (9)

FSX-430------50Co-28Cr-10Ni-7.5W-0.5C tested at 1000°C (10)

The composition of Haynes 188 is 44Co-28Cr-22Ni-15W-0.1C

Carbon concentration are higher and refractory metals content are lower in S-816 and FSX-430 than those in Haynes 188. This could lead to the reaction of hydrogen with free carbon (hydrogen attack) in the case of S-816 and FSX-430. The microstructures of FSX-430 tested at 1000°C consists of extensive fissures at grain boundaries and voids within the grains caused by decarburization (10). Hydrogen attack also occurs in S-816 tested in 815°C but not as serious as that of FSX-430 (9). Hydrogen attack is more pronounced for higher testing temperature. Testing temperature and alloying elements are the deciding factors in this kind of hydrogen degradation. 800°C is probably not high enough to activate the reaction of hydrogen with free carbon or extract carbon from existent carbides. The optical microstructures in Figure 13 exhibit similar microstructures and no hydrogen attack is observed. The TEM observations (Figure. 15 and Figure 18) also show similar dislocation and carbide morphology. The fractography observations in Figure 14 by SEM also do not show significant differences.

II. Mo-Re

The Mo-Re tested in 5% hydrogen + argon atmosphere seems to exhibit slightly higher creep rate than that tested in pure argon as in Figure 12. Stress exponents of 8 to 9 are observed which are indicative of power law break down region with dislocation glide

controlled deformation mechanism. The result appears to contradict the results of Flagella et al who observed that Mo-Re tested in argon and hydrogen atmosphere have the same creep behavior (19). The sample tested in hydrogen-containing atmosphere has a creep rate of 30 % faster than that tested in pure argon. This can be explained as follows:

Flagella tested Mo-Re at 2200°C in both argon and hydrogen and concluded that Mo-Re is immune to hydrogen degradation. However, If we refer to Mo-Re phase diagram in Figure 5 we see that Mo-Re is a single BCC phase at 2200°C but second phase χ precipitate when temperature drops below 1125°C. The misfit between matrix material and the χ phase might account for the observed degradation.

The testing temperature is the deciding factor for the operation of a particular deformation mechanisms. 2200°C is close to its melting temperature (2550°C) and diffusion is the main deformation mechanism. 800°C is low temperature for Mo-Re and dislocation glide is the main deformation mechanism. The increased creep rate may due to hydrogen enhanced dislocation mobility of Mo-Re.

The result reported previously (19) indicate that creep rate of Mo-Re tested at 2200°C varied. Flagella did several tests and concluded that they have the same creep behavior. The creep rates have variation of 20 to 80%. This indicates that our observed higher creep rate in the hydrogen-containing atmosphere may be within the scatter typically observed in creep tests.

6. CONCLUSIONS AND PLANS FOR FUTURE WORK

The testing results of Haynes 188 and Mo-Re in two atmospheres at 800°C do not show much difference in both mechanical properties and microstructures. However, as previously discussed the hydrogen effects are different at different temperatures, with different degradation mechanisms. Temperature is an important factor in determining the precise deformation mechanism. Our next step is the testing of materials in both atmospheres at 1000°C to evaluate their deformation mechanisms and hydrogen

degradation effects. Considerable delay has been encountered in the high pressure atmosphere testing at NASA/Marshall Space Flight Center because of technical problem with the set-up and lack of priority for our work.

7. REFERENCES

1. Alloy Phase Diagram, ASM Handbook, vol. 3, Dec. 1992.
2. Nelson, H. G. et al., Metall. Trans. vol. 3, p. 469, 1972.
3. Birnbaum, H. K. et al., Hydrogen in Metal, (ed. by Bernstein, I. M. and Thompson, A. W.), p. 303, ASM, 1974.
4. Hirth, J. P., Metall. Trans., Vol. 11A, p. 861, Jun. 1980.
5. Latanision, R. M. and Opperhauser, H. Jr. Hydrogen in Metal, (ed. by Bernstein, I. M. and Thompson, A. W.), p. 539, ASM, 1974.
6. Nelson, G. A. Hydrogen Plant Steel, Proc. Am. Pet. Inst., 29M(3), p. 163, 1949.
7. Mattsson, E. and Schueckher, F., J. Inst. Met. vol. 87, p. 241,1958-1959..
8. McCoy, H. E. Jr. Ph.D. Thesis, Univ. of Tennessee, 1964.
9. Klima, S. J., Nachtigall, A. J. and Hoffman, C. A., NASA Tech. Note D-1458, Dec. 1962.
10. Woodford, D. A. " An assessment of the Role of the Test Environment in Creep Rupture Life Prediction" Int'l Conf. on Engineering Aspect of Creep, p. 55, U. of Sheffield, 1980.
11. Sullivan, C. P., Varian, J. D. and Donachie, M. J. Jr., "Relation of Properties to Microstructure in Co-based Superalloys", p. 299, Source Book on the Materials for elevated-Temperature Application, ed. by Bradley, E. F., ASM, 1979.
12. Sandrock, G. D., Ashbrook, R. L. and Freche, J. C., The Effect of Silicon and Iron on Embrittlement of Cobalt-Based Alloy (L605), Cobalt, No. 28, p. 111, Sep, 1965.

13. Herchenroeder, R. B. and Ebihara, W. T. "In-Process Metallurgy of Wrought Co-Based Alloys", p. 313, Source Book on the Materials for elevated-Temperature Application, ed. by E. F. Bradley, ASM, 1979.

14. Greenfield, P. and Beck, P. A., JOM, Trans. AIME, Feb. 1956.

15. Wilson, C. G., Acta Cryst. vol. 16, p.724, 1963.

16. Davison D. I. and Brotzen, F. R., J. App. Phys., vol. 39, p. 7568, 1968.

17. Port, J. H. and Pontelandolfo, M. " Fabrication and Properties of Rhenium and Rhenium-Molybdenum Alloy" p. 555, Reactive Metals, ed. by Clough, W. R., AIME, 1959.

18. Sievert, A., Zeit. Phys. Chem. vol. 60, p. 129, 1907.

19. Flagella, P. N. and Tarr, C. O., Refractory Metal and Alloys IV, Research Development, vol. 2, ed. by Jaffee, R. I., Ault, G. M. and Maltz, J. and Semchyshen, M., p. 823, Gordon and Breach Science Publish, 1967.